University Oldenburg

ForWind - Wind Energy Systems

Design of Wind Energy Sytems

Author:
Jan Kämper
Florian Börgel

Supervisor:
Martin Kühn
Juan Jose Trujillo Quintero
Luis Enrique Vera Tudela Carreno

October 10, 2016

Contents

List of Figures

List of Tables

1 Introduction

This reports guides through the process of Design of Wind Energy Systems. The different phases are structured in so called CIPs. In the first CIP the main parameters of the turbine to be designed will be fixed and site conditions defined. Then in the second CIP the geometry of the blade will be computed according to Schmitz' and Betz' models. Performance curves are the subject of the third tutorial. CIP 4 treats the tower design. Impact of wakes and wind fields are investigated in CIP 5 before in the last CIP a fatigue load analysis (CIP 6a) and an extreme load analysis (CIP 6b) are carried out. During this project we have used a set of different tools and programming languages, among those: Matlab, Python, WT-Perf, Fast and Turbsim.

2 CIP 1: Selection of main parameters and rotor design

In CIP 1 we were asked to estimate the main parameters of our wind turbine model. In addition we also calculated the airfoil aerodynamics properties and defined the geometry of our blade. The following table shows the site specific conditions and the limitations for the design process of the wind turbine.

Name	unit	value
Airfoil profile set number	-	4
Design wind regime	-	Rayleigh
Target wind regime	-	High
Weibull A-factor (local)	m/s	9
Weibull k-factor (local)	-	2
Rated electrical power	kW	3500
Number of blades	-	3
Cut-in wind speed	m/s	3.5
Cut-out wind speed	m/s	25
Max. tip speed	m/s	82
Max. hub height – reference (*)	m	100
Max. blade length - reference (*)	m	60
Blade root length	m	5
Transmission	-	90

Table 1: Design parameters

2.1 Total conversion efficiency

The total conversion efficiency is used to calculate the amount of energy which can be extracted from the wind flow. Therefore it contains all loses due to mechanical and electrical conversions as

the corresponding c_p reference value. The c_p variable describes the maximum amount of energy which can be theoretical extracted from the wind. Taking all these losses into account we have the following equation for the total conversion efficiency:

$$\text{total conversion efficiency} = c_p * \nu_{el} * nu_{mech} = 0.4705 \tag{1}$$

2.2 Wind Power for nominal electrical power

The rated electrical power of the wind turbine is 3.500 kW. With the total conversion efficiency we computed in the last section we are now able to estimate how much wind power is needed to obtain nominal electrical power.

$$\text{total wind power} = \frac{\text{nominal power}}{\text{total conversion efficency}} = \frac{3500kW}{0.4705} = 7439.26kW \tag{2}$$

2.3 Rated wind speed

At rated wind speed the turbine is able to extract nominal wind speed. The following equation is used to calculate the power output of the wind turbine. It should be noted that resulting value had to be rounded up.

$$P_{rated} = 0.5 \cdot c_{total} \cdot \rho \cdot \pi \cdot R^2 \cdot V_{rated}^3 \tag{3}$$

where:

P_{rated} = rated electrical power
c_{total} = total conversion efficiency
ρ = density
R = reference max. blade length
V_{rated} = rated wind speed

This equation can be solved for V_{rated}:

$$V_{rated} = \sqrt[3]{\frac{2 \cdot P_{rated}}{\rho \cdot c_{total} \cdot R^2 \cdot \pi}} = 11m/s \tag{4}$$

2.4 Rotor radius

To calculate the rotor radius we used equation (3). Instead of solving for V_{rated} we solved for the blade radius.

$$R = \sqrt{\frac{2 \cdot P_{rated}}{c_{total} \cdot \rho \cdot \pi \cdot V_{rated}^3}} = 54m \tag{5}$$

With a hub diameter of 2.5 meters we end up with a blade length of 52.75 m.

2.5 Rotor area and specific rating

The rotor area is simply the area which is covered by the rotating blades. That leaves us with:

$$A_{area} = \pi * R^2 = 9161m^2 \tag{6}$$

Next we were asked to calculate the specific rating which is defined as:

$$rating = \frac{\text{electrical power}}{area} \tag{7}$$

We receive 382.06 W/m^2 as specific rating.

2.6 Rotor rated speed & design tip speed ratio

The design tip speed ratio is the ratio between maximum tip speed and rated wind speed of the turbine. The maximum tip speed for the wind turbine is $82m/s$ and the calculated rated wind speed is $11m/s$. That leads to a design tip speed ratio λ_d of **7.45**.

2.7 Annual Energy Production

Next, we calculated the rotor rated speed. The rotor rated speed in rotations per minute (rpm) is given by:

$$n = \frac{60s/min \cdot \text{ max. tip speed}}{2 \cdot \pi \cdot R} = 14.5rpm \tag{8}$$

2.8 Main aerodynamic properties

In order to estimate the design lift coefficient, the angle of attack and the drag coefficient we were given an excel sheet with the rotor design profile data for NACA-64-415 and NACA-64-421. Each sheet consists of 4 columns: angle of attack, lift coefficient, drag coefficient and thrust coefficient. According to the lecture, the optimal lift coefficient is defined as the maximum of the lift-to-drag ratio. Figure 1 shows the lift-to-drag ratio for different angles of attack (AOA).

The figures show that the highest lift-to-drag ratio occurs at low angles of attack. We identified the maximum at 3.0° for NACA 65-415 and 5.0°. For higher angles of attack the lift-to-drag ratio shrinks. However in practice there is another method to calculate the optimal design lift coefficient. In the further design we defined the design lift coefficient according to the following equation.

$$c_{l_{design}} = max(cl(max[\frac{c_l}{c_d}], 0.8 \cdot c_{l_{max}}) \tag{9}$$

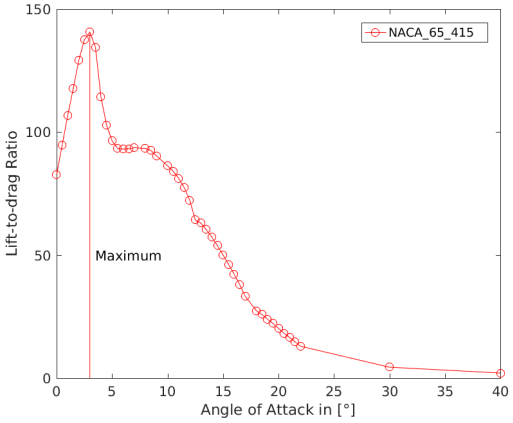

(a) Lift-to-drag ratio for NACA 65-415

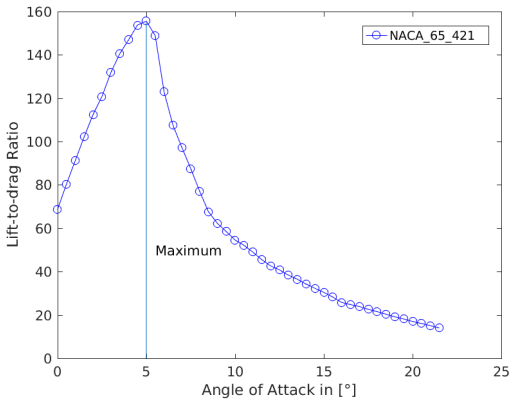

(b) Lift-to-drag ratio for NACA 65-421

Figure 1: Lift-to-drag ratio for different angle of attacks

The results are summarized in the following table:

NACA 65-415	α	c_l	c_d	c_m
80% method	10	1.345	0.016	0.071
lift-to-drag method	3.0	0.710	0.005	0.088
NACA 65-421	α	c_l	c_d	c_m
80% method	11	1.255	0.026	0.055
lift-to-drag method	5.0	0.952	0.006	0.092

Table 2: Main aerodynamic parameters

As the 80% method results in a higher lift coefficients for both profiles we selected the corresponding parameters according to the 80% method.

2.9 Annual Energy Production

The annual energy production is defined as

$$\text{total energy production} = \sum n_v \cdot p_v \tag{10}$$

with
n = number of hours
p = power curve
v = wind speed

With an assumed Rayleigh distribution figure 2 was calculated to show the wind speed distribution over a year.

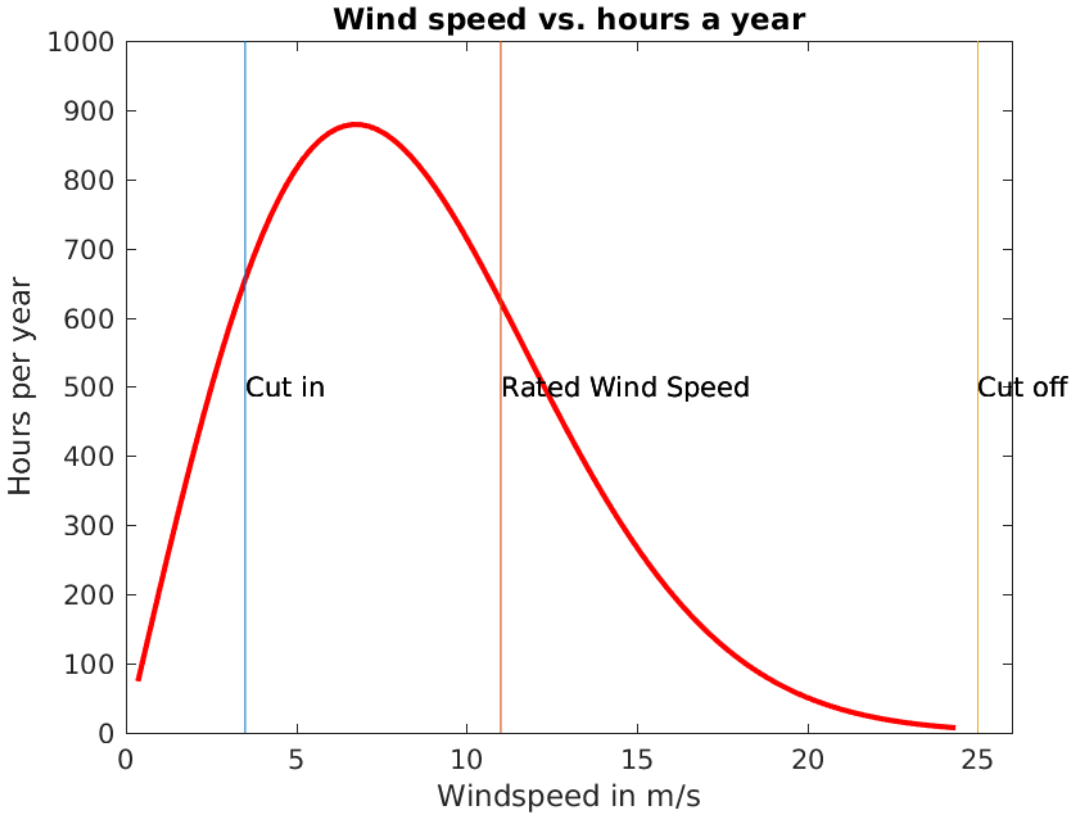

Figure 2: Wind speed vs. hours per year

In order to proceed with the calculation of the annual energy production the power curve was

also calculated, which is shown in the following figure.

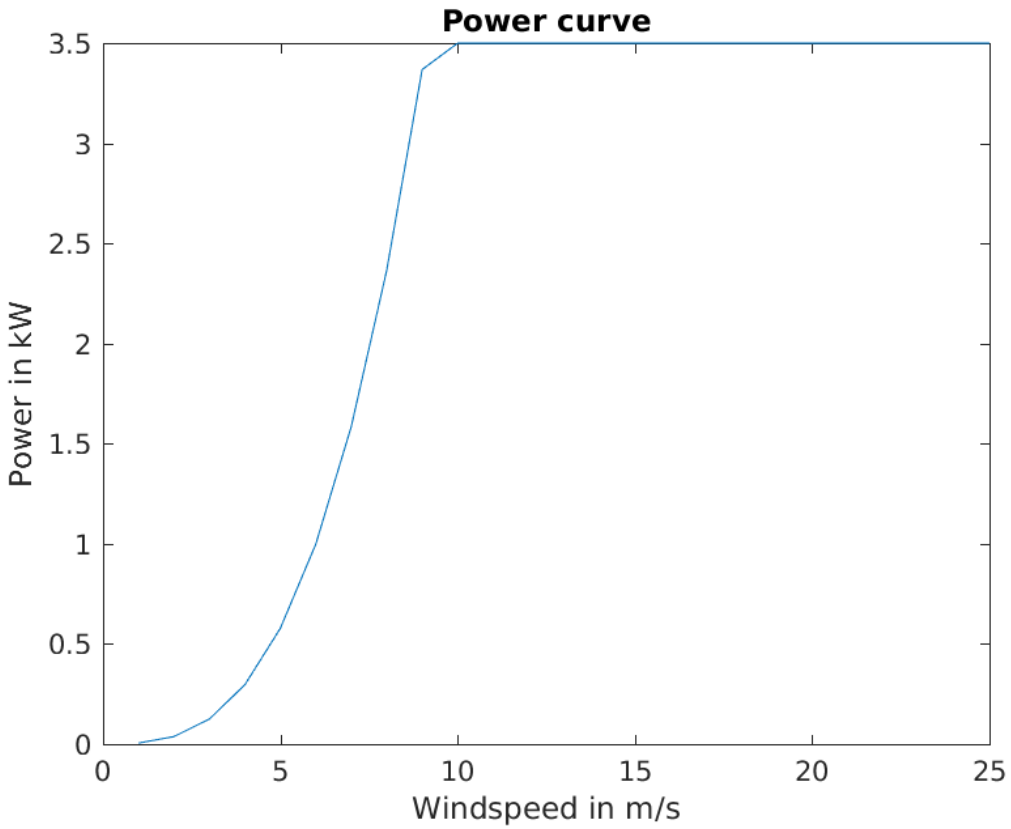

Figure 3: Power curve

With these two parameters we were able to calculate the annual energy production which can be extracted by integrating over the whole domain. Figure 4 shows the outcome. The annual energy yield is estimated at 18.325 kWh. In order to achieve the highest energy output it is necessary to guarantee a high availability of the turbine.

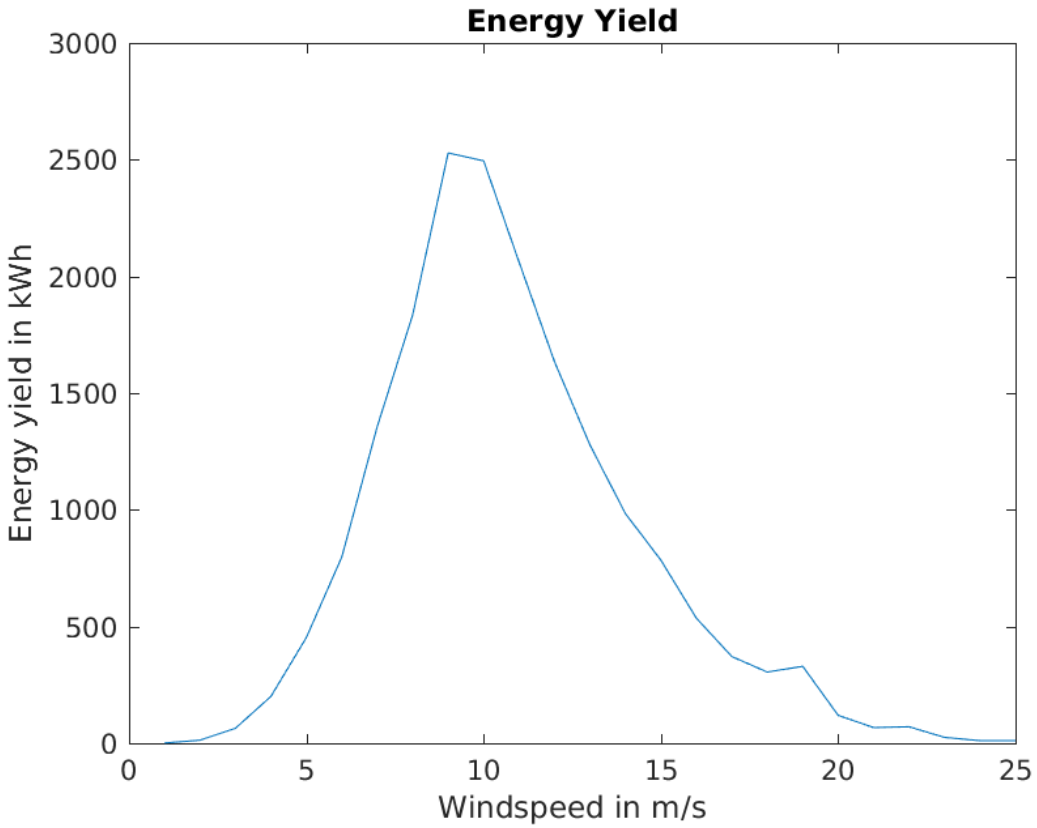

Figure 4: Annual Energy yield

3 CIP 2: Advanced BEM

In the first part of CIP 2 we designed the blade of the wind turbine. In the lecture we discussed two theories which are used to design the blade geometry. Betz and Schmitz theory both have different approaches to calculate the chord length and the twist angle. For the following steps it is import to keep in mind that the given blade consists of 10 blade elements, which are shown in the following figure.

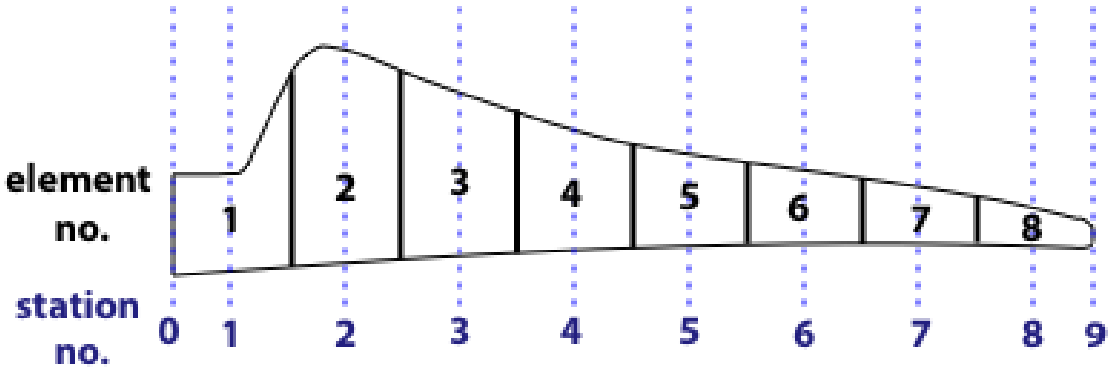

Figure 5: Blade Elements

3.1 Design your blade according to Betz theory

Betz theory estimates that the maximum of power that can be extracted from the wind is:

$$P_{betz} = \frac{16}{27} * P_{wind} \tag{11}$$

To understand why there is a certain limit, consider that if all energy coming from the wind movement through the turbine the speed afterwards would drop to zero then no new wind could get in and theenergy thus limited. The principle of Betz's law is derived from the principles of conservation of mass and momentum of the air stream following through and idealized 'actuator disk'. If we want to design the blade geometry according to this law, the power from the blade element theory has to equal P_{Betz}. This leads to the following equations which have been used for the further calculation.

Planform:

$$t(r) = 2\pi R \frac{1}{N} \frac{1}{\lambda_a \sqrt{(\lambda_a \frac{r}{R})^2 + \frac{4}{9}}} \tag{12}$$

Twist angle:

$$\alpha(r) = \arctan(\frac{2}{3} \frac{R}{r\lambda_a}) \tag{13}$$

$$\alpha_{twist} = \alpha(r) - \alpha_a \tag{14}$$

Using the parameters from CIP 1, we calculated the chord length and the twist angle for each blade segment. An overview is shown in table 3.

Station number	1	2	3	4	5	6	7	8	9
Dist.(rotor center) m	4.547	11.141	17.734	24.328	30.922	37.516	44.109	50.703	54.000
Dist.(blade root) m	3.297	9.891	16.484	23.078	29.672	36.266	42.859	49.453	52.750
NACA 65-415									
Chord length m	10.963	5.989	3.957	2.932	2.324	1.923	1.639	1.428	1.342
Twist angle deg	36.725	13.436	5.233	1.228	-1.123	-2.665	-3.752	-4.559	-4.890
NACA 65-421									
Chord length m	11.749	6.418	4.240	3.142	2.490	2.061	1.757	1.531	1.438
Twist angle deg	35.725	12.436	4.233	0.228	-2.123	-3.665	-4.752	-5.559	-5.890

Table 3: Blade design according to Betz theory

3.2 Design according to Schmitz

The blade design according to Schmitz uses the following equations:
Planform:

$$t(r) = \frac{16\pi r}{N c_l} \sin^2(\frac{1}{3}\alpha_1) \tag{15}$$

Twist angle:

$$\alpha(r) = \frac{2}{3}\alpha_1 \tag{16}$$

$$\alpha_{twist} = \alpha(r) - \alpha_a \tag{17}$$

where

$$\alpha_1 = \arctan(\frac{R}{\lambda_a r b}) \tag{18}$$

Using the same approach of the previous section we end up with the following results, shown in table 4.

Station number	1	2	3	4	5	6	7	8	9
Dist.(rotor center) m	4.547	11.141	17.734	24.328	30.922	37.516	44.109	50.703	54.000
Dist.(blade root) m	3.297	9.891	16.484	23.078	29.672	36.266	42.859	49.453	52.750
NACA 65-415									
Chord length m	6.184	5.063	3.671	2.812	2.262	1.887	1.616	1.412	1.328
Twist angle deg	28.589	12.022	4.812	1.054	-1.210	-2.714	-3.783	-4.579	-4.906
NACA 65-421									
Chord length m	6.628	5.426	3.934	3.013	2.424	2.022	1.732	1.514	1.424
Twist angle deg	27.589	11.022	3.812	0.0548	-2.210	-3.714	-4.783	-5.579	-5.906

Table 4: Blade design according to Schmitz theory

The final blade is designed according to Schmitz theory by a combination of profile 1 and profile 2. The first station has got a cylindrical shape. For stations 2-5 the thinner profile is used, for stations 6-8 the thicker profile is used.Table 5 gives more detail about the design rotor blade.

Station number	1	2	3	4	5	6	7	8	9
	Cylinder	65-421	65-421	65-421	65-421	65-415	65-415	65-415	65-415
Blade m	3.297	9.891	16.484	23.078	29.672	36.266	42.859	49.453	52.750
Chord length m	6,628	5,426	3,935	3,014	2,425	1,887	1,617	1,413	1,329
Twist angle deg	27,590	11,022	3,813	0,055	-2,211	-2,715	-3,783	-4,580	-4,907

Table 5: Final blade design according to Schmitz

3.3 Corrections to BEM

For the further evaluation of the designed blade we used the blade element momentum theory (BEM). BEM helps to estimate the local forces acting on a wind turbine blade. The first assumption of this theory is the actuator disk model, where we consider a wind turbine in a stream tube, as shown in figure 6.

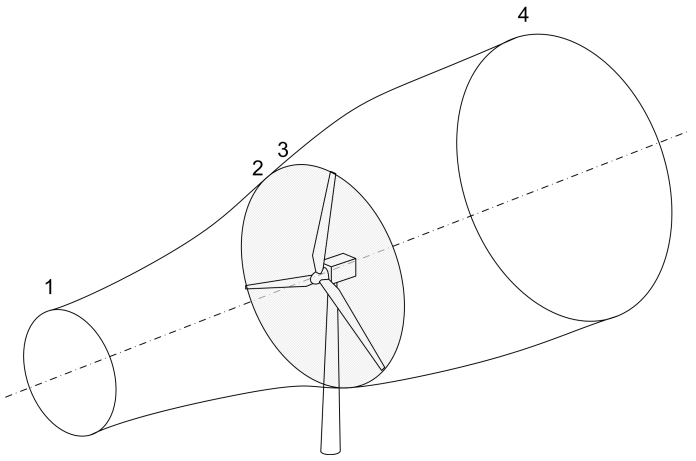

Figure 6: Actuator disk model

Therefore we assume a closed system, which must obey momentum conservation. The rotor is moved by the incoming wind and angular momentum is induced. The wind is also influenced and is slowed down. The change in velocity is described by the induction factor a.

$$v_2 = v_1(1 - a) \tag{19}$$

In the following we first introduce the BEM algorithm and discuss some of the corrections which have to be consider when designing a wind turbine. It should be noted that these corrections are not used in the further design process because the application of the BEM is very complex and is done by specially designed programs.

3.3.1 BEM algorithm

The BEM algorithm is an iterative process and is limited by a convergence test. The following figure shows the main idea of the BEM algorithm.

3.3.2 Prandtl factor

The BEM theory by itself fails to represent all of the occurring effects which have to be considered. One major effect is the finite number of blades. The BEM theory calculates an uniform induction factor over each rotor ring, but in reality the local solidity decreases toward the tip and is not uniform over the ring. To deal with these errors the Prandtl correction is applied. The effects are shown in the following figure.

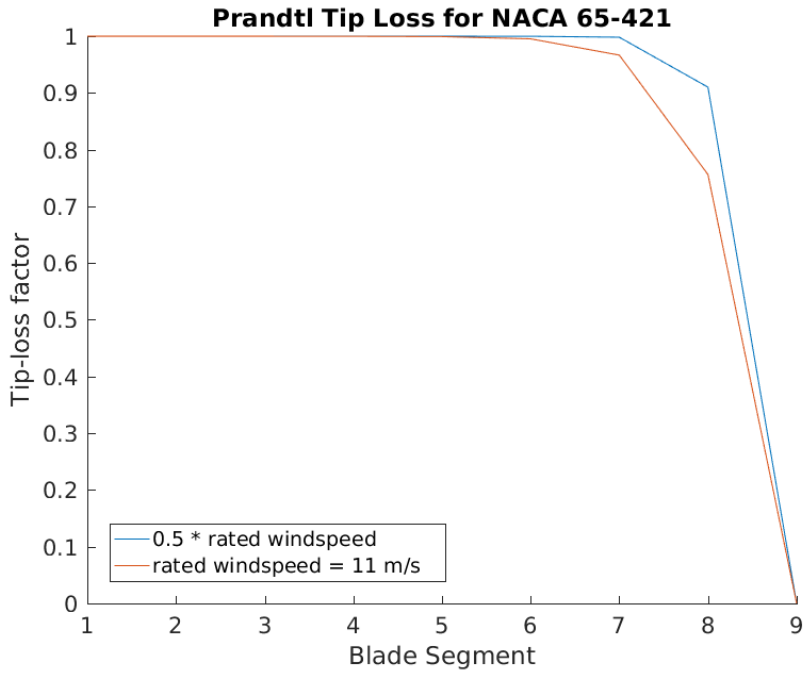

Figure 7: Prandtl Tip los

The figure shows that the tip-loss factor decreases with increasing r/R ratio. There are not big differences for alternating wind speeds. However it seems that higher wind speeds have a slightly bigger influence on the tip losses.

3.4 3D corrections

Measurements show that sometimes stall turbines have significant higher power in stall range than calculated. This is due to 3D effects which are not considered by 2D models. To deal with this problem, different corrections terms can be applied. In the following two different models are shown. Figure 8 shows the correction by Chaviaropoulus and Hansen and figure 9 the correction by Snel.

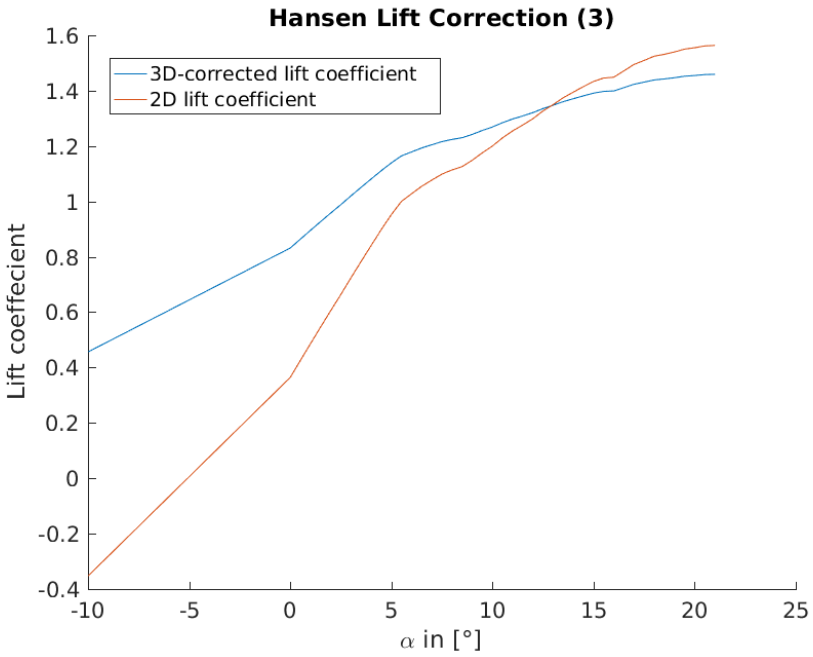

Figure 8: Hansen 3D Correction

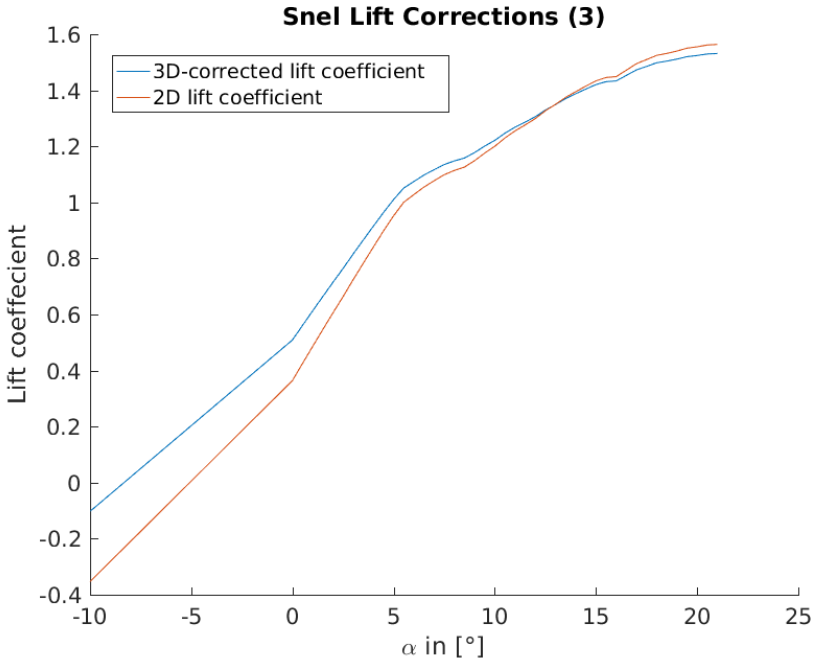

Figure 9: Snel 3D correction

3.5 Pitching moment

We calculated the pitching moment at the different blade elements according to the following formula:

$$M = C_m \cdot A \cdot c \cdot \rho \cdot v^2 \cdot 0.5$$

The total pitching moment can be obtained by adding up the moments of all blade elements. The results for the two different wind speeds (v_{rated} and $0.5v_{rated}$) are as follows:

$$M(5.5m/s) = 15.881Nm$$
$$M(11m/s) = 278.705Nm$$

Figure 10 depicts the pitching coefficients in dependance of the angle of attack.

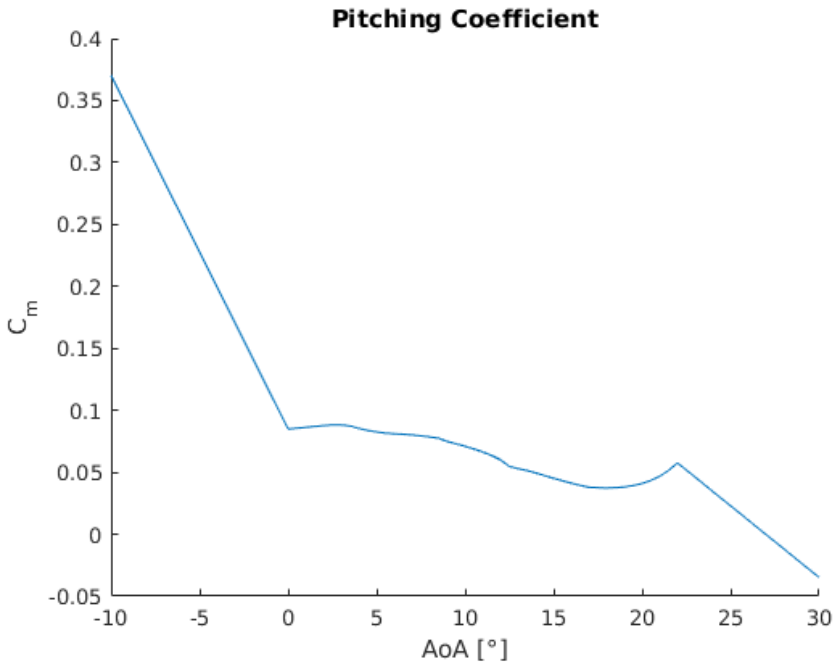

Figure 10: Pitching coefficient

4 CIP 3: Performance Curves

4.1 Introduction

In this section we analyzed the designed turbine under different pitch angles and tip-speed ratios. The design process of a wind turbine differs from turbine to turbine. In order to compare wind turbines non dimensional coefficients are used. These do not depend on factors like size or wind conditions. The most common coefficient is the power coefficient c_p. Further we used the torque coefficient c_q and the thrust coefficient c_t. These coefficient are defined as:

$$c_p = \frac{P}{0.5 * \rho A v^3} \qquad c_t = \frac{T}{0.5 \rho A v^2} \qquad c_q = \frac{Q}{0.5 \rho A v^2 * R}$$

where:
c_p = Power coefficient
c_t = Thrust coefficient
c_q = Torque coefficient
p = Power
ρ = Density
A = Area
v = Wind speed
R = Rotor radius

4.2 WT_Perf

To compute the non dimensional parameters a program called WT_Perf is used. WT_Perf uses blade-element momentum (BEM) theory to predict the performance of wind turbines. [1]. It also takes different correction algorithms into account, e.g. Prandtl's tip-loss and hub-loss model. WT_Perf can be used from the operating system's command prompt. In order to use WT_Perf we configured the input file by updating the 'Turbine Data' section and implementing the calculated blade geometry. WT_Perf also needs the aerodynamic data of the airfoils. We were able to use the provided data here. Last we defined the range of pitch angle and tip-speed ratio according to the tasks of CIP 3.
The following code-snippet gives an idea of the input file structure:

[1] WT_Perf_Users_guide.pdf

```
------ Turbine Data ----------------------------------------------------------
     3                 NumBlade:                  Number of blades.
 62.18                 RotorRad:                  Rotor radius.
  1.25                 HubRad:                    Hub radius.
 -3.0                  PreCone:                   Precone angle, positive downwind.
  5.0                  Tilt:                      Shaft tilt.
  0.0                  Yaw:                       Yaw error.
  100                  HubHt:                     Hub height.
    8                  NumSeg:                    Number of blade segments.

   RElm    Twist    Chord    AFfile   PrntElem
  3.808   26.530    6.988      1      FALSE
 11.424    9.594    5.407      1      FALSE
 19.040    2.661    3.832      1      FALSE
 26.656   -0.866    2.906      1      FALSE
 34.272   -1.967    2.171      2      FALSE
 41.888   -3.354    1.806      2      FALSE
 49.504   -4.335    1.544      2      FALSE
 57.120   -5.066    1.348      2      FALSE
```

4.3 Comparison

As already mentioned we configured the input file according to CIP 3. The generated output file contains values for the power coefficient c_p, thrust T and torque Q. For task 3.2 we wrote a small python-program which examines the data and plots the results for the three different non dimensional coefficient mentioned in the introduction of CIP 3: c_p, c_t and c_q. Since WT_Perf only writes the power coefficient we had to calculate c_t and c_q. Note that the coefficients are functions of $c_t(\lambda), c_q(\lambda)$. The following figures display the results for c_p, c_t and c_q with a tip-speed ratio λ from 1 to 20 and pitch angles of 0,5,10,15,20 and 30 degree. The curves are calculated at rated rotor speed (12.59 rpm).

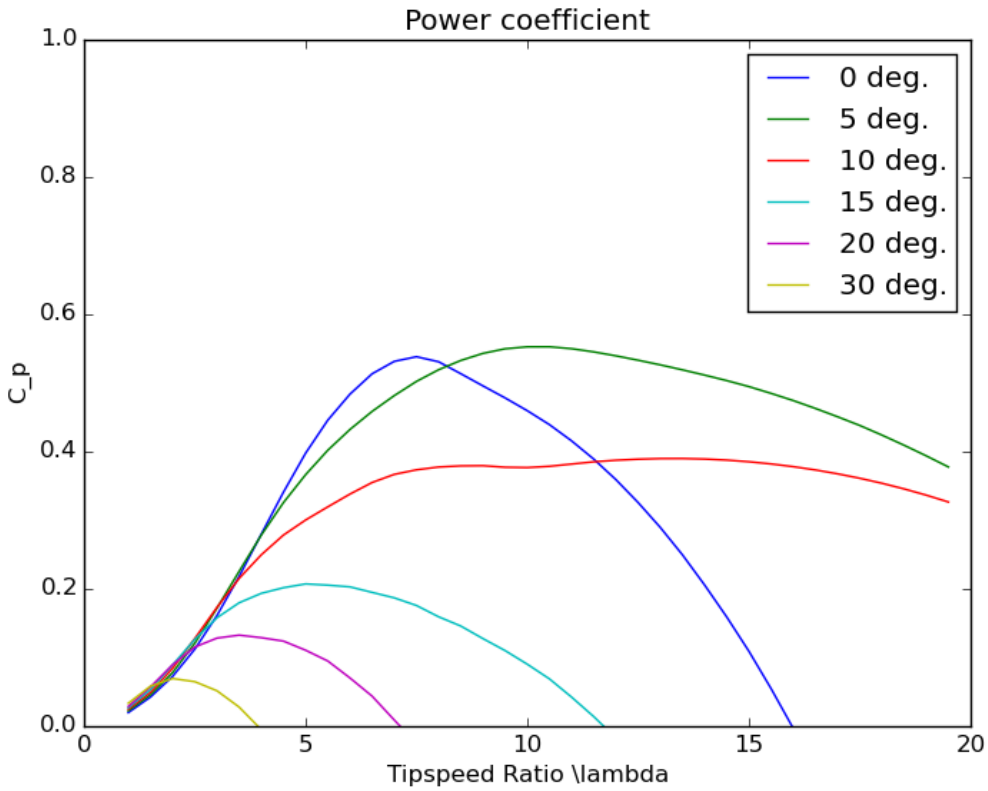

Figure 11: Power coefficient

The $c_p - \lambda$ curve shows different power coefficients at different tip-speeds and pitch-angles. Regarding the maximum for c_p at each curve we identify that they appear at different tip-speed ratios. At pitch angle 5° the maximum c_p is at 0.564 which is very close to the theoretical maximum of 0.592.

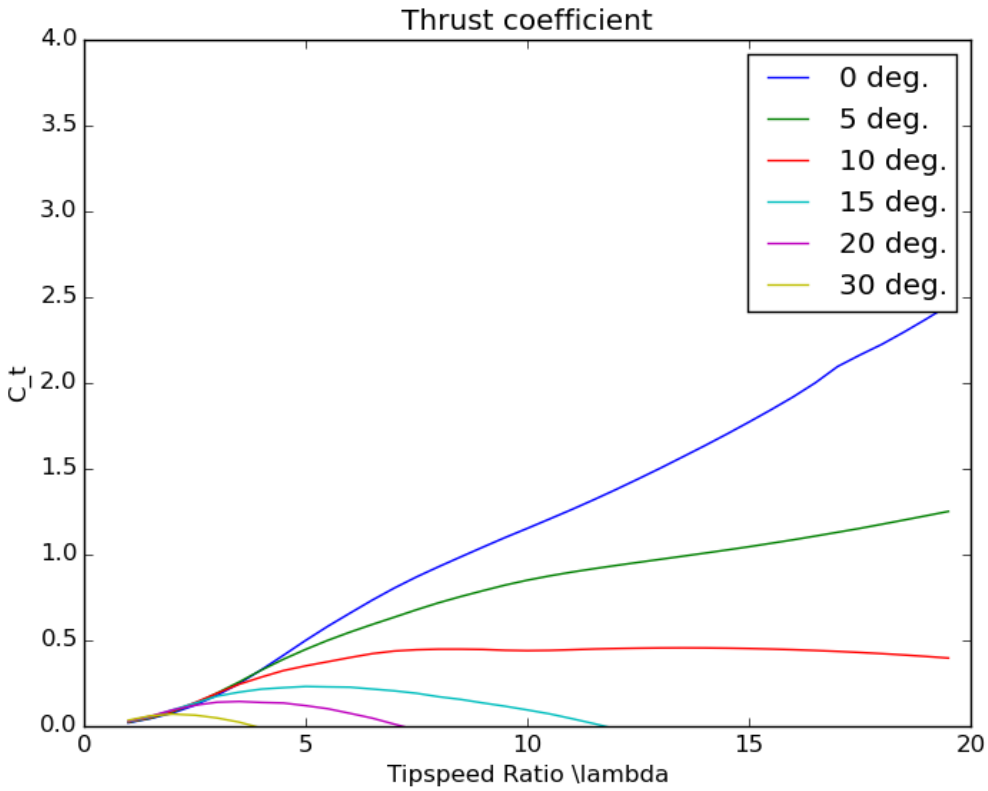

Figure 12: Thrust coefficient

Figure 12 shows the behavior of the thrust coefficient. From 0° to 10° the thrust coefficient reaches high values. For higher pitch angles the resulting thrust coefficient is significantly lower and is equal to zero for higher tip speed ratios. The thrust is directly applied at the tower and can be decreased by increasing the pitch angle.

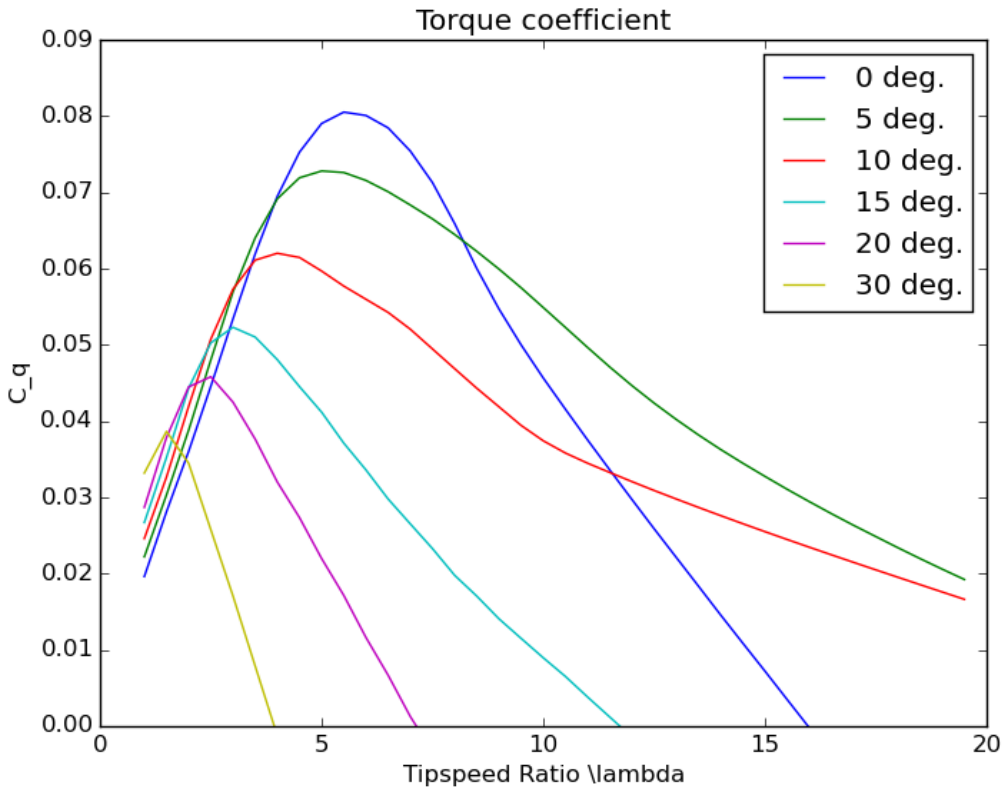

Figure 13: Torque coefficient

Figure 13 shows the torque coefficient for different pitch angles. Compared to the $c_p - \lambda$ the maximums are shifted to the left and decrease with increasing pitch angle.

In the following the simulated results are compared to the corresponding curves from the literature[2]. Figure 14 shows a power curve from literature. The maximum c_p is close to 0.52 at zero degree pitch and design tip speed ratio. The results from figure 11 is somewhat similar with the maximum at 0.554. Also the shape of pitch angles 0, 10, 20 and 30 degree of the designed turbine have a similar shape compared to the power curve from the literature. The designed turbine seems to overestimate the c_p for higher tip speed ratios at pitch angle 5° and 10°. According to the literature lower c_p values should be assumed.

[2]Gasch, R.: Wind Power Plants - Fundamentals, Design, Construction and Operation, 1st Edition, Solarpraxis AG, Berlin, 2002

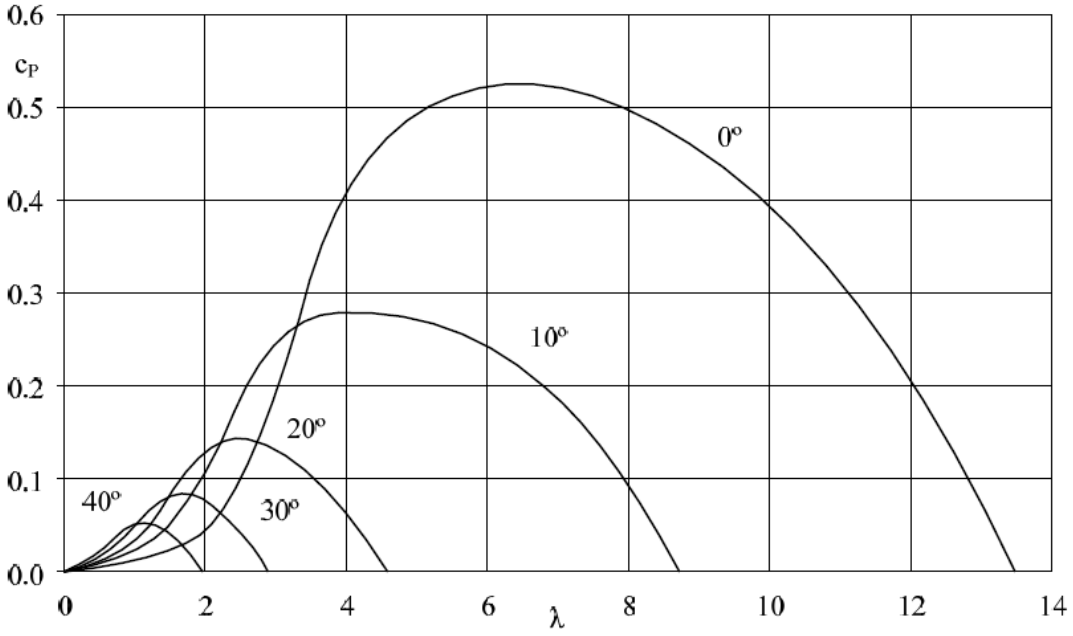

Figure 14: Power coefficient from literature

The same comparison has been done for the thrust coefficient. Figure 15 shows the expected outcome predicted by the literature. It can be seen that the thrust coefficient for the designed turbine looks very similar in it's shape compared to the thrust coefficient shown in figure 15. For high pitch angles the curve reaches zero quickly. Lower pitch angles lead to an increasing thrust coefficient for higher tip speed ratios.

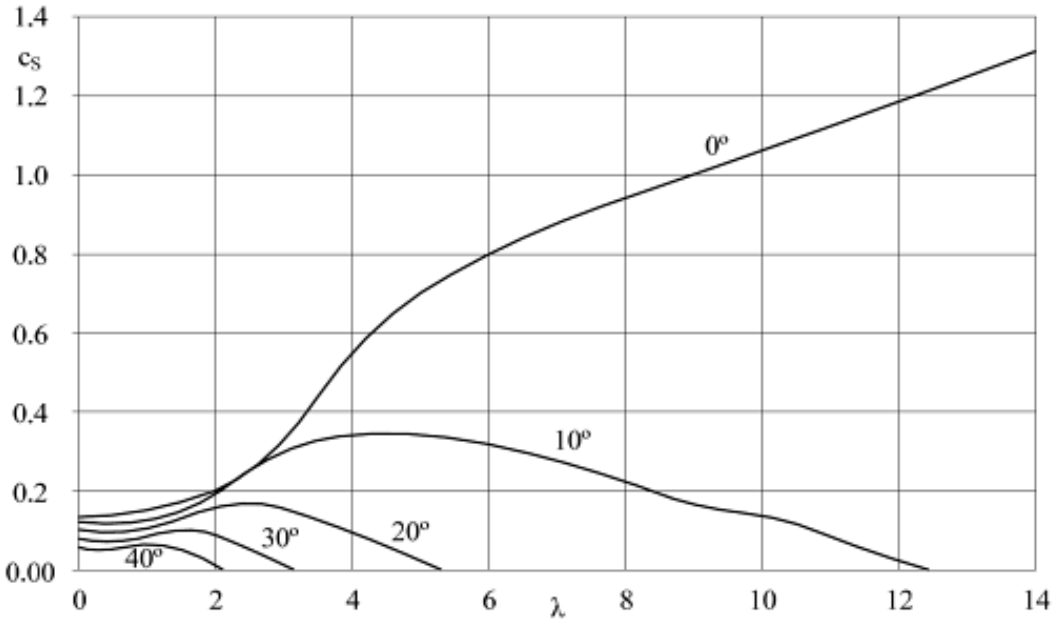

Figure 15: Thrust coefficient from literature

At last the predicted torque coefficient was evaluated in figure 16. The designed turbine shows the same deviation that was already seen in the power curve. Pitch angles 5 and 10 degree seem to be a little bit off for higher tip speed ratios.

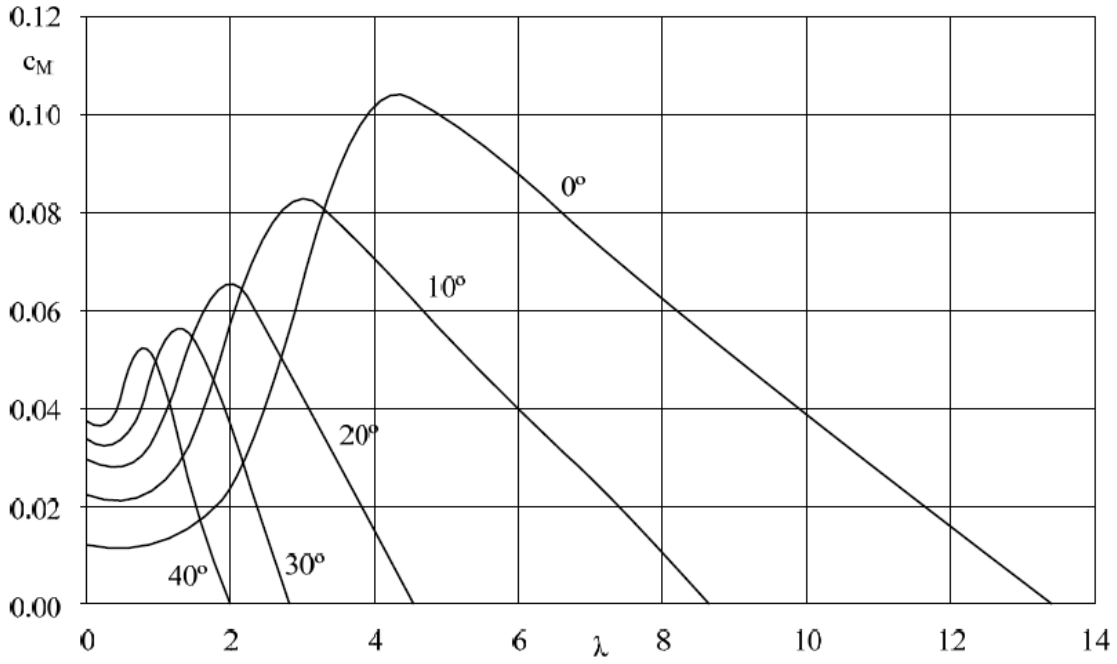

Figure 16: Torque coefficient from literature

4.4 Rotor rated speed

In task 3.4 we were asked to calculate the resulting rotor speed for a rated wind speed of 9 m/s. For the calculation we used our design tip speed ratio:

$$\lambda = \frac{\Omega R}{v} \tag{20}$$

$$n = \frac{60\lambda v}{2\pi R} = 10.07 rpm \tag{21}$$

4.5 Operation conditions

Again we used WT_Perf to calculate the resulting operation conditions below rated wind speed. The input parameters are: v = 9 m/s, design top speed ratio $\lambda = 8.2$ and rotational speed $n = 10.07$ rpm. The results are shown in the following table:

v	rotor speed	c_p	c_t	c_q	P
m/s	rpm	-	-	-	kW
9	10.07	0.544	0.825	0.033	2054.846

4.6 Coefficients

According to Betz, the wind turbine should be able to extract 7618 kW. However the rated power of the wind turbine is lower than the power which could be extracted. Therefore pitching is needed. The resulting c_p can be calculated as follows:

$$c_p = \frac{3500000}{0.5 \cdot 1.225 \cdot \pi \cdot 62.18^2 \cdot 12^3} = 0.272 \tag{22}$$

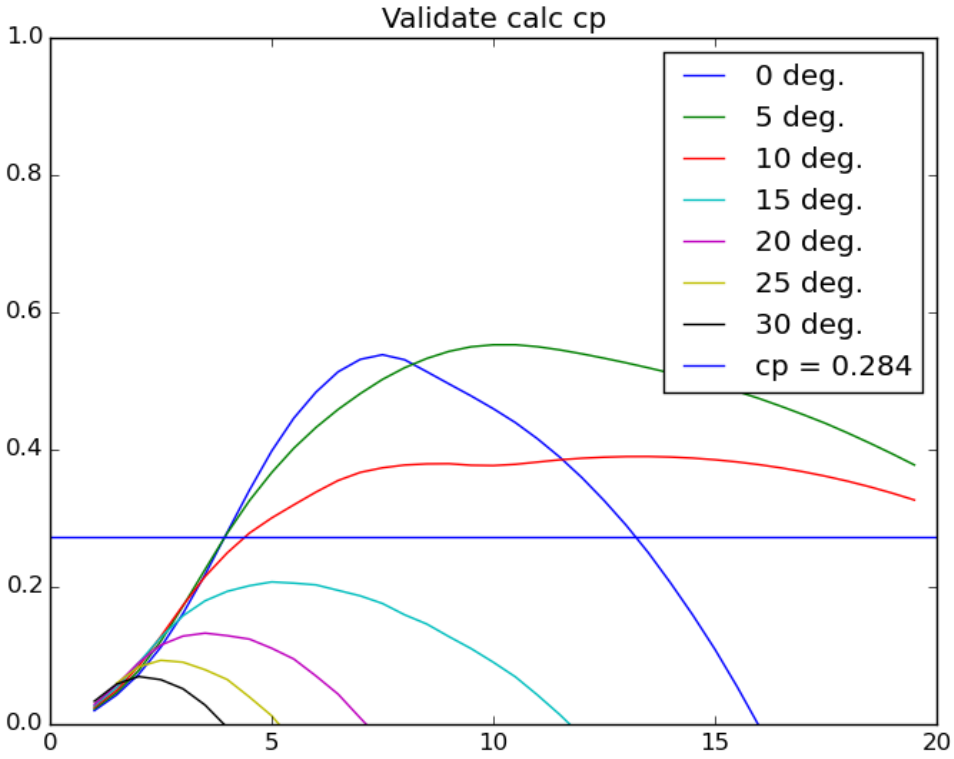

Figure 17: Validation of c_p
The resulting c_p corresponds to a tip speed ratio of 5 with a pitch angle of 10°

4.7 Rotor speed

$$n = \frac{60\lambda v}{2\pi R} = 9.21 rpm$$

It can be seen, that for conditions below rated wind speed it is still possible to achieve a high power coefficient. The calculated power coefficient for 9 m/s is 0.544. If the wind speed is higher than the rated wind speed the power coefficient drops significantly. This is due to the limited capacity of the generator. Not all kinetic energy of the wind can be transformed into electrical energy and pitching is required to protect the generator. In both cases the rotations per minute are below rated rotor speed. Therefore the most efficient possibility to design a turbine is to make it variable. A constant tip speed ratio can be achieved, which leads to a high power coefficient.

5 CIP 4: Tower design

In this part of the Design project a modal analysis for tower design will be carried out and evaluated with respect to economical factors. For this purpose the following parameters are relevant:

$$\begin{aligned}
\Omega_{rated} &= 14.5rpm \text{ (rotor rated speed)} \\
D &= 5m \text{ (tower diameter)} \\
E &= 211000000000\frac{N}{m^2} \text{ (elastic modulus)} \\
l &= 100m \text{ (hub height)} \\
m_{top} &= 323000kg \text{ (nacelle and rotor mass)} \\
\rho &= 7850\frac{kg}{m^3} \text{ (material density)}
\end{aligned}$$

5.1 Eigenfrequency

For tower design resonances of excitation frequencies from the rotating blades must be taken into account. The Eigenfrequency of the tower can thus be obtained by adding a 10% safety margin to the rotor rated speed which represents the maximum stationary rotor speed:

$$f_0 = \Omega_{rated} \cdot 1.1 = \frac{14.5}{60}Hz \cdot 1.1 = 0.2658Hz$$

5.2 Design range

The design range of our turbine is a classical soft-stiff design which results in large wave excitation but allows variable speed turbine design since resonances with tower eigenfrequencies at frequencies lower than rated rotor speed are avoided. There are a few other common design approaches one of which is the soft-soft design where the eigenfrequency lies within the resonance range of the rotor. In this case certain rotor frequencies have to be excluded in order to avoid resonances.

5.3 Wall thickness

The wall thickness t can be computed from the following equations:

$$f_0 \cdot 2\pi = \sqrt{\frac{k}{m_{top} + 0.25 m_{tower}}} \tag{23}$$

$$k = \frac{3E\pi D^3 t}{l^3 8} \tag{24}$$

$$m_{tower} = \rho \pi D t l \tag{25}$$

By substituting Equations (22) and (23) into (21) we obtain the following equality which can be fed into Matlab in order to solve for the only unknown t:

$$0 = \sqrt{\frac{3E\pi D^3 t}{l^3 8 \cdot (m_{top} + 0.25\rho\pi D t l)}} - f_0 \cdot 2\pi$$

Extract from Matlab code used to solve for variable t:

```
t=1;
func = @(t) sqrt(3*E*pi*D^3*t/(l^3*8*(mTop+0.25*rho*pi*D+t*l)))-f0*2*pi;
t = fsolve(func,t);
```

The resulting value for the wall thickness is $t = 0.0318m$. The tower mass is then $m_{tower} = 391730kg = 391.73t$. The material cost for this tower would thus be of 195870 €, assuming a price of 500 €/t. Obviously a thicker tower wall leads to a higher price overall (linear increase). As depicted in Figure 18 a thicker wall leads to a higher Eigenfrequency of the tower as well. However, in this case the relationship is not a linear one due to the exponent of 0.5 in the formula. Hence, a thicker wall results in a higher Eigenfrequency but the increase is only significant for wall thicknesses up to $0.1m$. Above that the cost increase does not justify the gain in Eigenfrequency because wall thickness and costs are proportional but the Eigenfrequency is under-proportional.

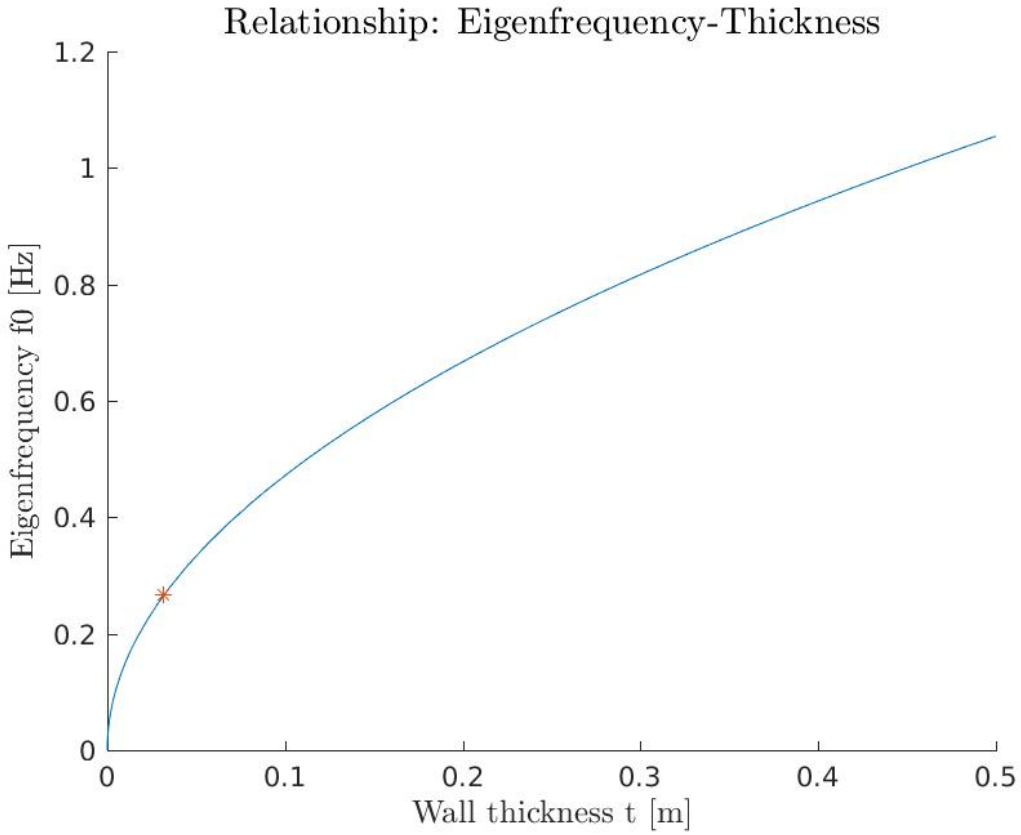

Figure 18: Effect of wall thickness on Eigenfrequency

5.4 Campbell diagram

The Campbell diagram is depicted in Figure 19. The red line shows the computed Eigenfrequency of the tower and the circles mark resonance cases for certain rotor speed values due to periodic excitations. For example the dashed blue line (1Ω) represents the 1P excitation (unbalance from the rotation), the second blue line (3Ω) represents the periodic excitation caused by a tower shadow of one of the three blades.

The operational range of the rotor with respect to tower Eigenfrequencies must thus be kept within certain limits. By designing the tower wall thickness with adding a 10% safety margin to the rotor rated speed we can are on the safe side and avoid 1P excitations (intersection point of the Ω line with the red line). It must further be excluded during operations that any of the other intersection points occur, e.g. 3Ω line with red line. Some rotational speed ranges must thus be

excluded in operation in order to avoid any resonances.This analysis however only considers tower resonances. A complete evaluation must take into account more resonances as well, e.g. 1st blade edgewise and 1st blade flapwise eigenfrequencies.

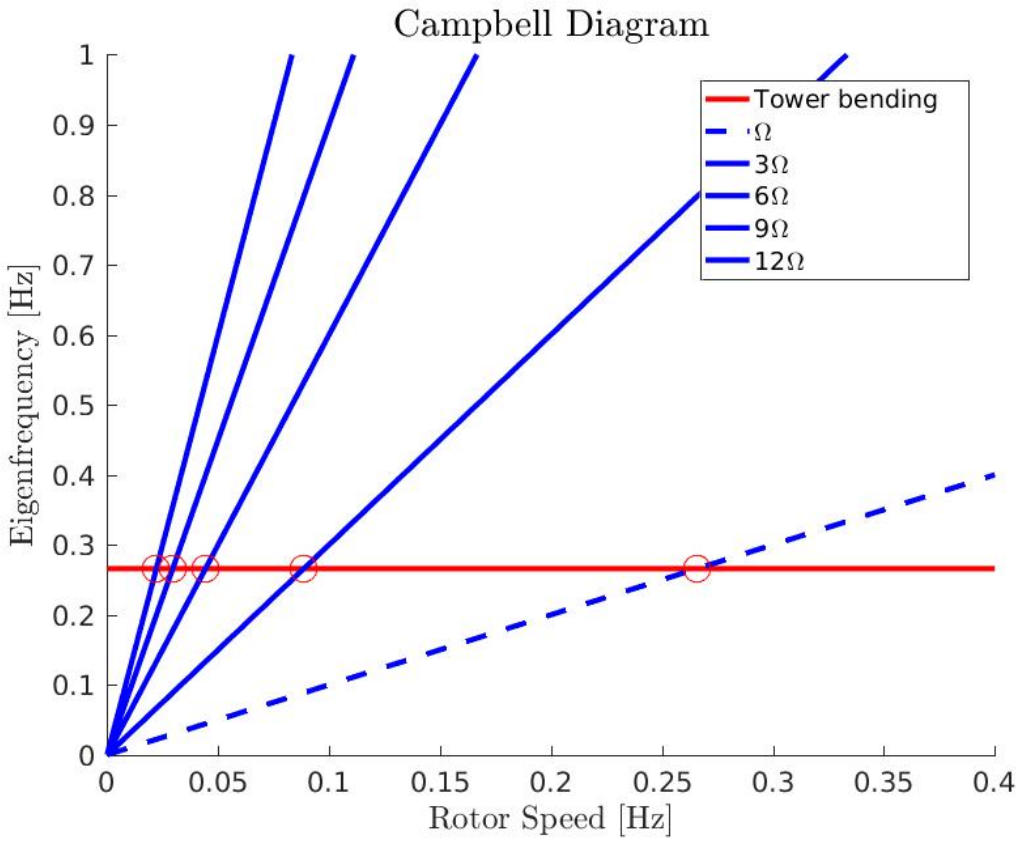

Figure 19: Campbell Diagram

6 CIP 5: Wind fields and wake modeling

6.1 Wind speed distribution: Rayleigh

Assuming a wind class type I-B gives per definition a reference wind speed of $V_{ref} = 50m/s$ and a reference turbulence intensity of $I_{ref} = 0.14$. The Rayleigh distribution as a special case of Weibull where the shape parameter has a value of $k = 2$. The average wind speed can be derived from the reference wind speed as follows: $V_{ave} = V_{ref}/5 = 10m/s$. From this we can derive the scale parameter via $V_{ave} = \lambda \cdot \sqrt{\frac{\pi}{2}}$ resulting in $\lambda = 7.97m/s$. The corresponding wind speed distribution

following a Weibull law with $\lambda = 7.97m/s$ and $k = 2$ is depicted in Figure 20. Frequencies were multiplied with 8760 in order to represent the absolute number of hours per year. Three crucial wind speeds are highlighted in the diagram: Cut-In speed ($3.5m/s$), Rated speed ($11m/s$) and Cut-Out speed ($25m/s$). These three limits define the operational conditions of the turbine: Between Cut-In and Rated speed the turbine is operating in partial load, between rated speed and Cut-Out the turbine is operating under full load. Beyond these limits the turbine is not operating.

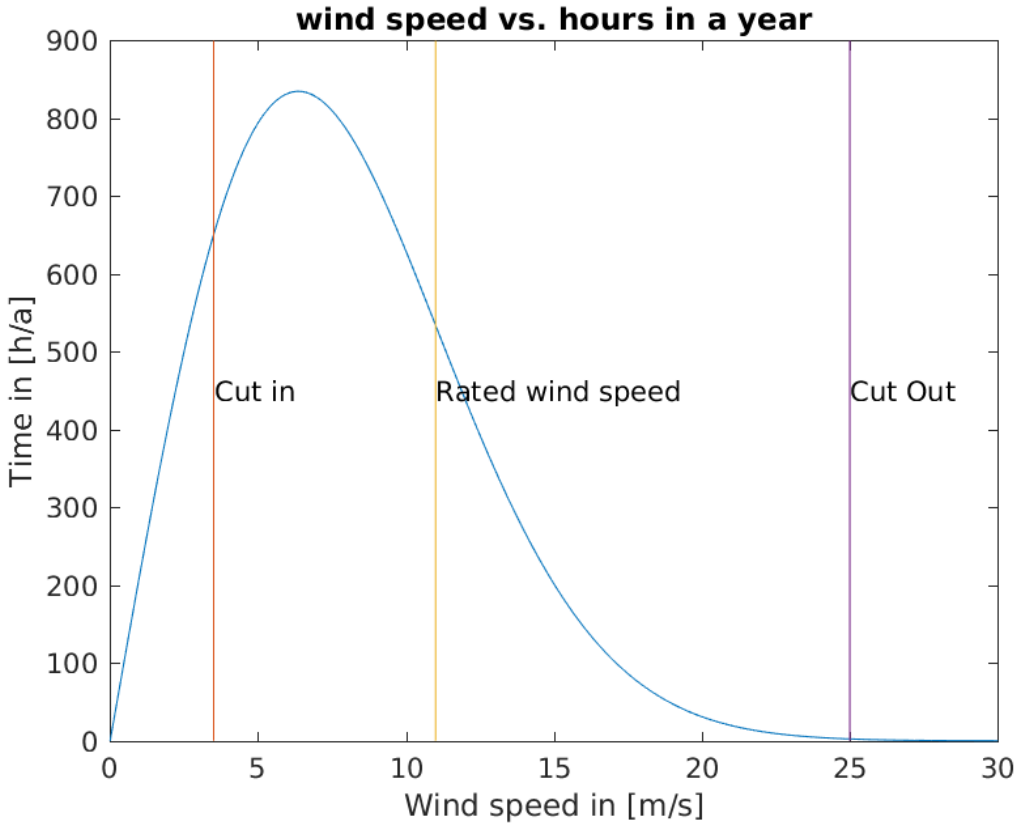

Figure 20: Wind speeds vs hours per year

6.2 Power curve and AEP

The power produced depending on the wind speed can be obtained from the following formula:

$$P(v) = 0.5 \cdot \rho \cdot \nu \cdot \pi \cdot R^2 \cdot v^3$$

Wind density is fixed at $\rho = 1.225$, the total conversion efficiency is given as $\nu = 0.4705$ and the rotor swept area is $\pi \cdot 54^2 m^2$. For wind speeds above rated wind speed the power output of the turbine will be constant. The corresponding power curve is depicted in Figure 21.

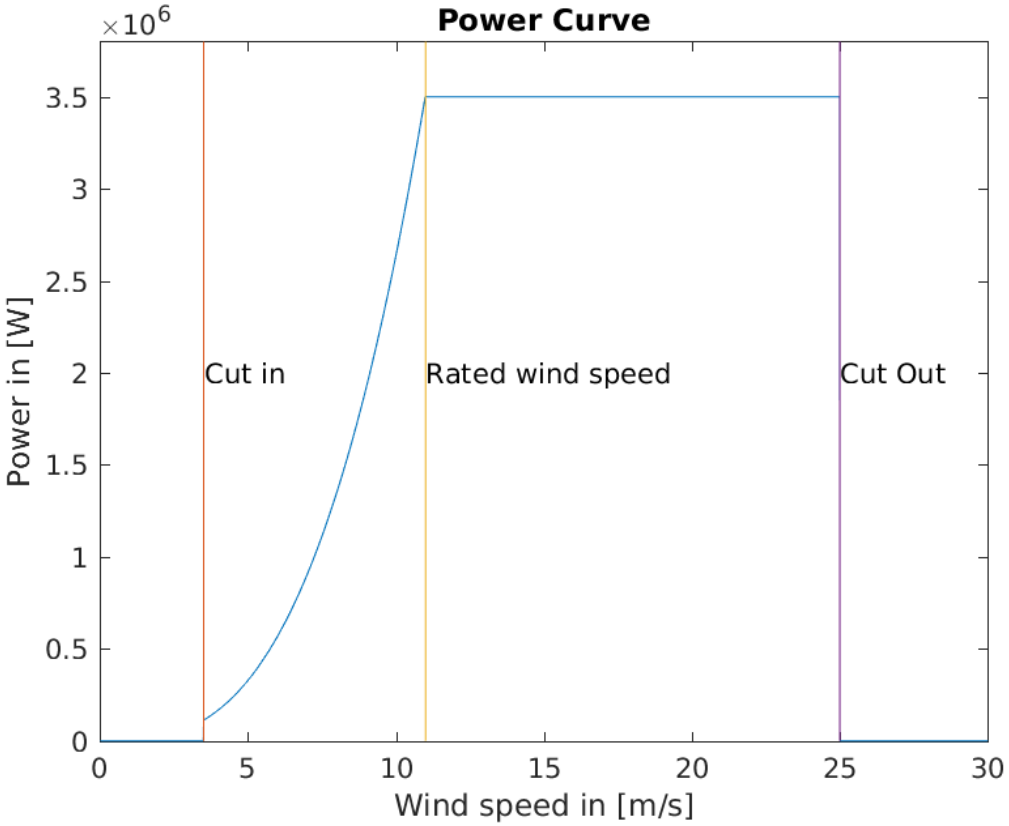

Figure 21: Power curve

Combining the wind speed distribution from Figure 20 and the power curve from Figure 21 enables computing the annual energy production. We multiply the number of hours for each wind speed with the power output at that specific speed and integrate this over all relevant wind speeds. The result corresponds to the area under the curve in Figure 22.

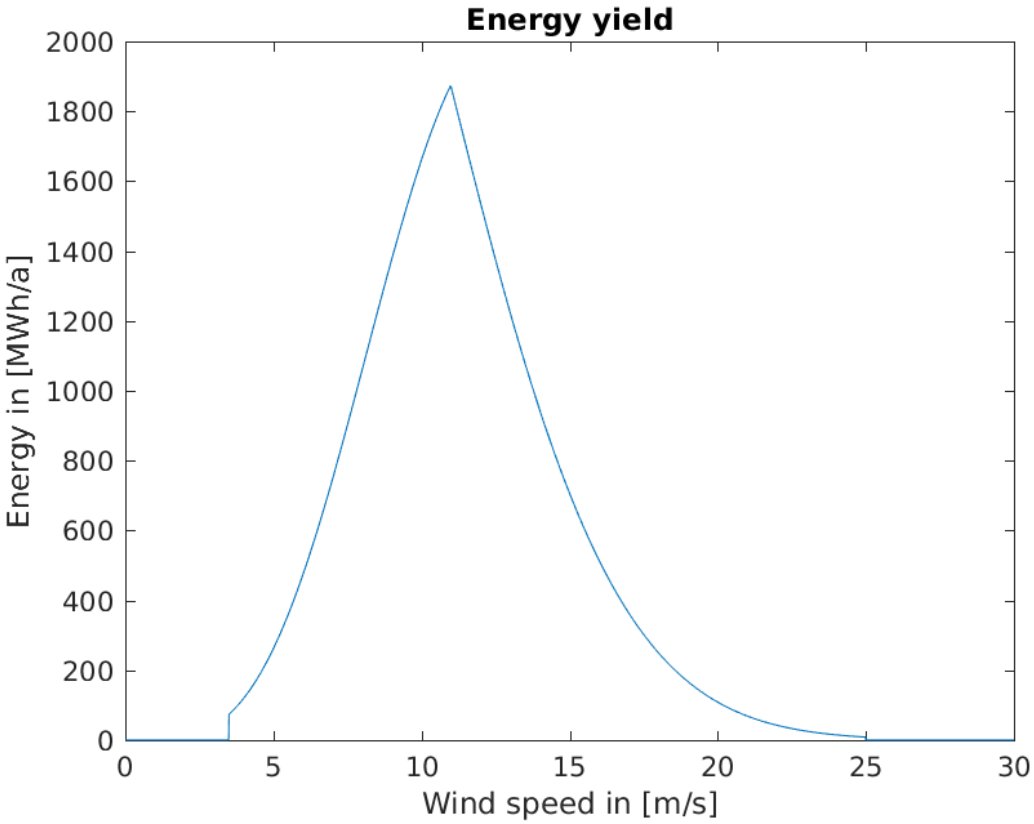

Figure 22: Energy yield for different wind speeds

Here, the total AEP is of about 11.099 GWh. For a 100% availability and a feed-in tariff of 0.08 €/kWh the revenue is thus of approximately 887930€. If we assume an availability of only 95% the corresponding revenue lies around 843530€which results in a loss of nearly 45000€in one year.

6.3 Turbulence intensity under free stream conditions

Applying the normal turbulence model we calculated the turbulence intensity for different wind speeds. The wind class type is I-B which defines a reference intensity of $I_{ref} = 0.14$. The result for the four given wind speeds is shown in Table 6.

v	$5m/s$	$10m/s$	$15m/s$	$25m/s$
I	0.2618	0.1834	0.1573	0.1364
Operational condition	partial	partial	full	full

Table 6: Turbulence intensity according to NTM at different wind speeds

From Figure 22 in the previous section we have seen that the biggest portion of the AEP of the turbine is contributed by wind speeds around rated wind speed. At higher wind speeds less energy is produced because these wind speeds simply are much less frequent due to the distribution, especially speeds of 20m/s and higher are insignificant to the AEP. However, wind speeds around 5m/s or 15m/s do have an impact. Regarding the turbulence intensity shown above we can then conclude that there is no direct relation between turbulence and power output.

6.4 Wind fields with TurbSim

Using TurbSim we generated wind fields for the given conditions, see Figure 23.

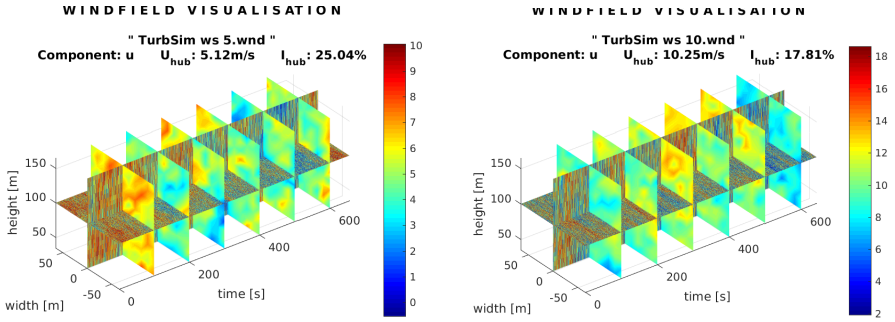

(a) At 5m/s

(b) At 10m/s

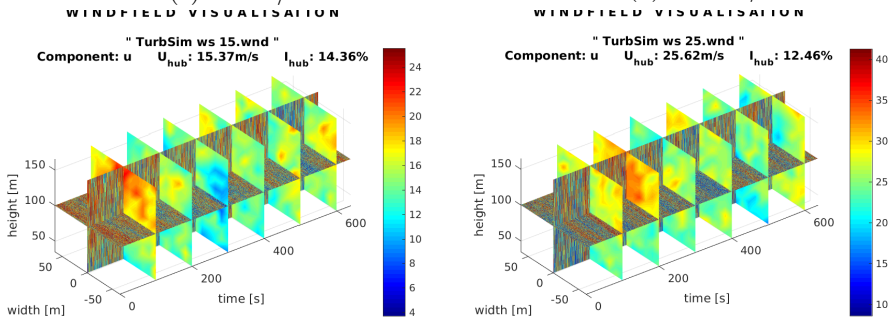

(c) At 15m/s

(d) At 25m/s

Figure 23: Wind fields by TurbSim

6.5 Wake modeling with Frandsen

We now use Frandsen's model in order to analyze wakes. Two different setups will be evaluated: One with distances between the turbines of 4 times the rotor diameter, and one with 8 times the rotor diameter. The result for the four given wind speeds is shown in Table 7. The results for the NTM model have been carried over in order to compare these to the wake results.

v	$5m/s$	$10m/s$	$15m/s$	$25m/s$
$\mathbf{4 \cdot d}$	0.2667	0.1867	0.1594	0.1370
$\mathbf{8 \cdot d}$	0.2621	0.1827	0.1562	0.1349
NTM	0.2618	0.1834	0.1573	0.1364

Table 7: Turbulence intensity according to NTM at different wind speeds

Clearly the turbulence intensity is lower for the case of larger distances ($8 \cdot d$) for all wind speeds. However, the difference between the free stream turbulence and the case of larger distances is only marginal. For a wind speed of 5 m/s the turbulence intensity is lower in the free turbulence model, but for all other wind speeds the Frandsen model leads to lower turbulences then the free stream model.

The complete dataset for all wind bins and all three cases is visualized in Figure 24. It is not easy to recognize, but by looking closely we find that the order $8 \cdot d$, NTM, $4 \cdot d$ from lowest to highest turbulences holds for all wind bins above 10 m/s.

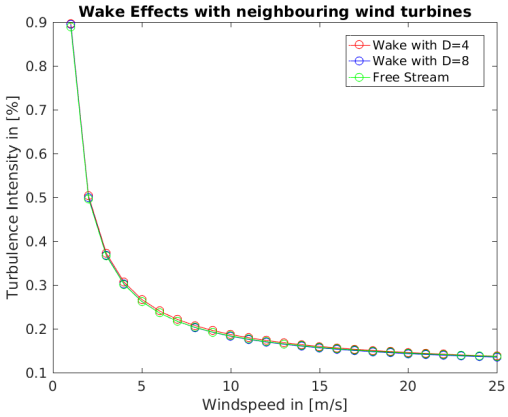

Figure 24: Turbulence intensity in different setups

We generated wind fields for wake conditions with both layouts as well since these will be used later. A comparison of the wind field under free stream conditions with the wind field under wake condition ($4 \cdot d$) for $v = 5m/s$ is shown in Figure 25. The two wind field do not diverge very much,

but the computed turbulence intensity differs considerably (0.2504 vs 0.2544).

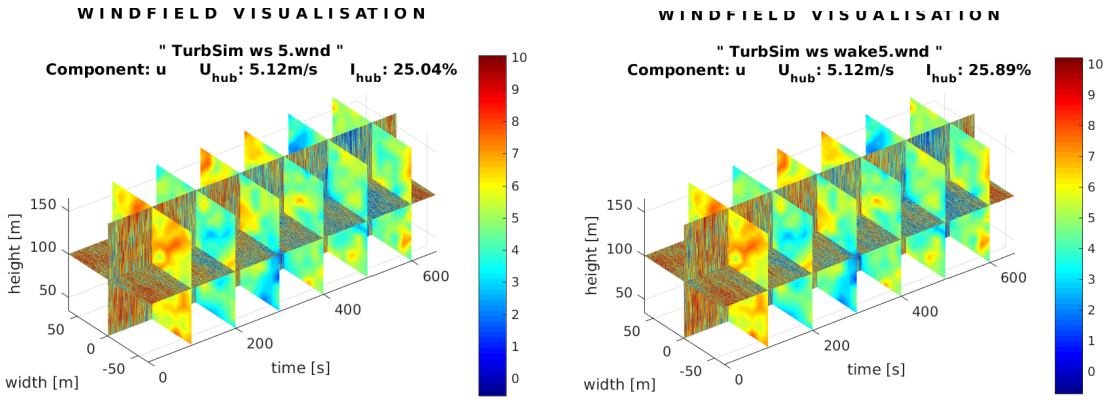

(a) Wind field for Free stream at 5m/s

(b) Wind field for Wakes with $4 \cdot d$ at 5m/s

Figure 25: Free stream vs Wake conditions

6.6 Possible faults

Failures can occur with respect to electrical components and the turbine control. These failures must be simulated in order to ensure structural integrity of the turbine. Possible faults are defect pitch or yaw actuators, which lead to the turbine being unable to reduce or increase forces and might cause a breakdown. Also it could be that sensors are defect and supply wrong data which would result in a fatal mis-behavior of the turbine. Likewise the drive train and gearbox might be affected by broken parts causing severe failure of the turbine if not handled correctly. The generator of a turbine can be subject to electromechanical problems, e.g. torque scaling fault, overheating, asymmetries etc.

7 CIP 6a: Fatigue loads

7.1 FAST

The wind fields from the previous chapter will now be used to run simulations with FAST for fatigue analysis. We use the same wind speeds of 5,10,15 and 25m/s and free stream conditions.

Figure 26 shows the signals for the four variables (tower side-to-side, tower fore-aft, blade flapwise and blade edgewise) at a wind speed of $v = 5m/s$. Units are kNm. The corresponding signals for higher windspeeds are analogue with a different scaling and different frequencies.

We can see that the tower fore-aft bending moments are highest while side-to-side tower moments and blade edgewise moments are moderate. The oscillations are very regular in the case of the edgewise bending moments of the blade. For the other cases we see different maximums and minimums and some evolution in the course of the signal.

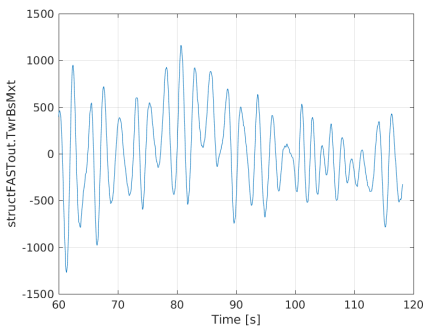

(a) Tower side-to-side bending moments

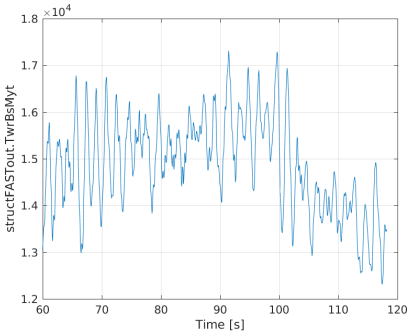

(b) Tower fore-aft bending moments

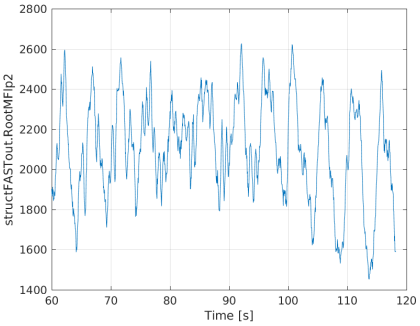

(c) Blade flapwise bending moments

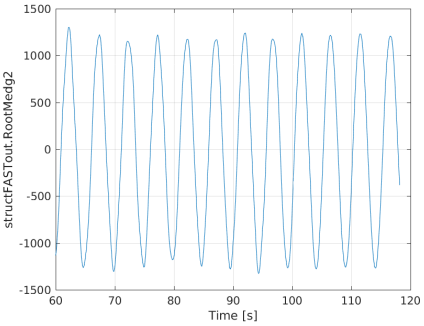

(d) Blade edgewise bending moments

Figure 26: Time series of bending moments for different variables at $v = 5m/s$

7.2 Damage equivalent loads under free stream condition

The DELs under free stream conditions for tower and root can be found in Table 8. Damage equivalent loads are used to represent the cyclic loads of a time series in one numeric value. We find confirmation for the result from the previous section: Highest loads occur in case of the tower fore-aft and edgewise blade bending moments. The loads increase with the wind speed over-proportionally for all variables.

v	$5m/s$	$10m/s$	$15m/s$	$25m/s$
Tower side-to-side	811.645	1466.761	2112.274	4974.035
Tower fore-aft	2382.669	2990.821	3862.967	6328.944
Blade edgewise	1924.045	2387.446	2432.449	2552.909
Blade flapwise	738.816	1426.071	1765.008	2353.317

Table 8: DELs under free stream conditions

7.3 Damage equivalent loads under wake condition

The DELs under wake condition for tower and root can be found in Table 9.

neighboring distance	$4 \cdot d$				$8 \cdot d$			
v	$5m/s$	$10m/s$	$15m/s$	$25m/s$	$5m/s$	$10m/s$	$15m/s$	$25m/s$
Tower side-to-side	775.607	1404.149	2087.209	5419.259	810.116	1445.473	2132.343	5356.443
Tower fore-aft	3050.375	3695.06	3620.304	6162.187	2651.542	2677.856	3516.175	5957.573
Blade edgewise	1940.040	2419.468	2416.637	2555.216	1923.647	2397.627	2436.092	2560.151
Blade flapwise	814.974	1445.028	1701.446	2308.930	791.422	1351.939	1721.214	2299.36

Table 9: DELs under wake condition

Comparing the DELs in the three different settings (free stream and wake with $4 \cdot d$ and $8 \cdot d$) in Figure 27 we can see that for the edgewise blade DELs there is no notable difference between the three settings. For the flapwise blade moments however the DELs are lowest for the setting with wakes and a $8 \cdot d$ distance and highest for a $4 \cdot d$ distance while the free stream setting lies in the middle. Regarding the tower DELs the differences are more clear, especially in the case of fore-aft bending. Here again the $8 \cdot d$ distance setting has lowest DELs at most wind speeds (except 5m/s) while the free stream setting has lower DELs then the $4 \cdot d$ setting for moderate wind speeds. The fact that the $8 \cdot d$ distance case results in lower DELs then the $4 \cdot d$ distance case is as expected as we saw in the previous chapter that the turbulence intensity is lower for the setting with larger distances between neighboring turbines. However, we would have thought that the free stream setting results in even lower DELs since the turbulence intensity was shown to be lower with the NTM model then in the Frandsen model.

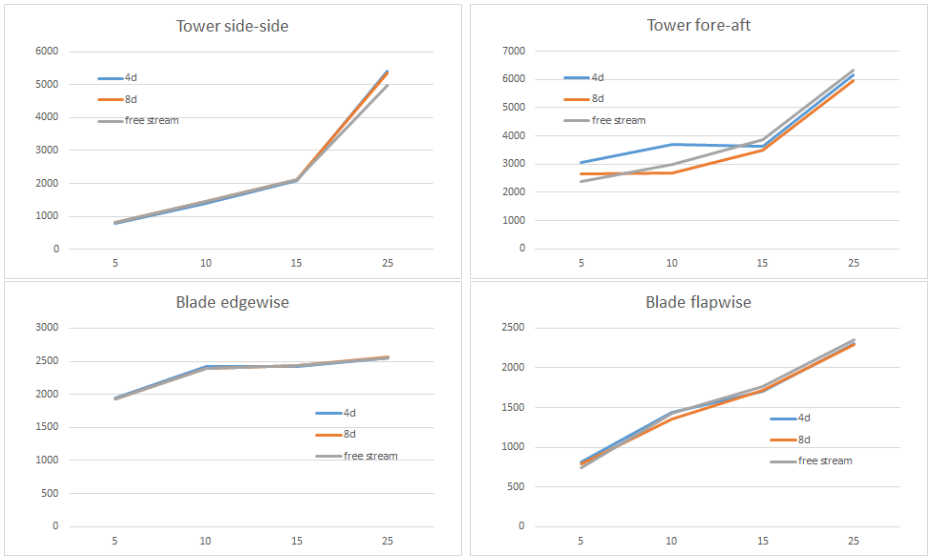

Figure 27: Comparison of the DELs

7.4 Statistical max/min sensor values

The statistical max and min values of the sensors analyzed above for all settings can be seen in Table 10.

	Tower side-side		Tower fore-aft		Blade flapwise		Blade edgewise	
	Min	Max	Min	Max	Min	Max	Min	Max
NTM 5m/s	-1272	1163	12310	17310	1452	2626	-1328	1304
NTM 10m/s	-629.6	1635	9931	21010	778.8	3110	-1678	1285
NTM 15m/s	-2701	3865	4047	20430	-306.5	3192	-1798	1580
NTM 25m/s	-8513	8904	732.7	23270	-1855	2903	-2001	1684
4d, 5m/s	-1271	1504	4610	19290	1016	2861	-1332	1314
4d, 10m/s	-2666	2637	8794	40330	766.2	5109	-1807	1775
4d, 15m/s	-2481	3642	3418	19770	-291.7	3247	-1802	1609
4d, 25m/s	-8523	9251	260.2	22730	-1844	2894	-1992	1710
8d, 5m/s	-1183	1529	5393	19760	1024	2908	-1330	1306
8d, 10m/s	-2912	2818	8901	38050	774.3	4984	-1866	1838
8d, 15m/s	-2397	3576	3439	19730	-272.9	3206	-1804	1602
8d, 25m/s	-8490	8621	1003	23480	-1889	2921	-2021	1684

Table 10: Max and mins of sensor values

7.5 Power spectral density

For the blade flapwise bending moment and for the tower fore-aft bending moment under wake conditions (with $8 \cdot d$ distance) the power spectral density plots can be found in Figure 28. Two different wind speeds of 5 m/s and 25 m/s were chosen. The overall pattern of the spectral density is similar in all cases. Frequencies below 1 Hz are most powerful but occur less then higher frequencies. Higher wind speeds leads to higher frequencies and flattens the spectral profile a little.

This tower was designed with an Eigenfrequency of $0.2658Hz$. There is no obvious effect on the power spectral density of the Eigenfrequency. However, the power spectral density in all cases has these spikes which should be in same way linked to the Eigenfrequency of the system components, i.e. multiples of the blades flapwise and towers eigenfrequencies.

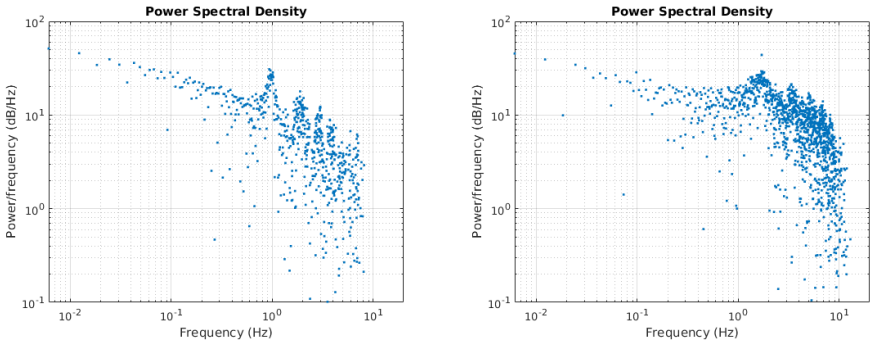

(a) Blade flapwise at 5 m/s

(b) Blade flapwise at 25 m/s

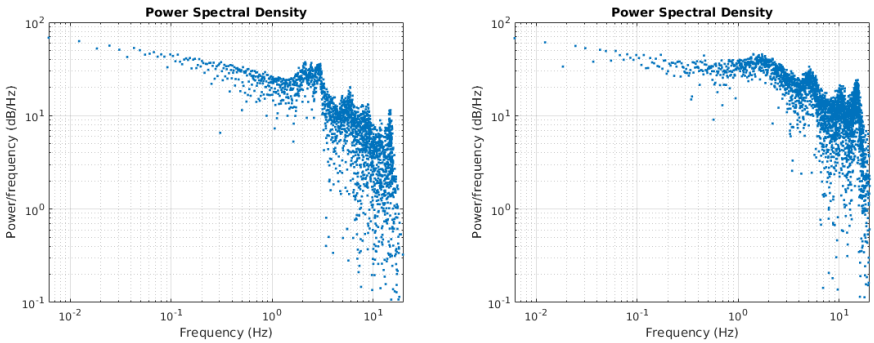

(c) Tower fore-aft at 5 m/s

(d) Tower fore-aft at 25 m/s

Figure 28: Power spectral density plots

8 CIP 6b: Extreme loads

8.1 Extreme conditions

- Load case 1.3:
  Power production under the ETM (extreme turbulence model). This load case is important because extreme turbulences can damage the turbine's components much more than normal turbulence which reduces lifetime. These conditions must thus be simulated

- Load case 1.5:
  Power production under the EWS (extreme wind shear). Extreme wind shear occurs when there is a high vertical (or horizontal) wind speed profile, which means that wind speeds differ considerably depending on the location on the rotor area. Blades are loaded non-linearly and also the drive-train can receive varying loads which might cause damages.

- Load case 2.1:
  Control system fault or loss of electrical network. During production (NTM) a non-functioning control system or a turbine without electrical network is in extreme conditions because missing control or even erroneous control of the turbine, e.g. wrong pitch angel, can result in production losses and even failure or damages of the turbine.

- Load case 6.1:
  The turbine is in parked position and the underlying wind model is EWM (extreme wind) with a 50-year recurrence. This practically means an exceptionally strong gust which occurs statistically only once within 50 years and might only last a few seconds (3 seconds). Clearly, such an extreme condition can pose severe problems to a turbine including breaking of components.

- Load case 8.1:
  The turbine is transported, assembled, maintained or repaired. Even under the NTM and wind speeds defined by the manufacturer these steps in the lifetime of a turbine must also be simulated because wrong handling during any of these steps can damage parts of the turbine.

8.2 Simulation of extreme load cases 1.5 and 2.3

Now we will simulate two extreme load cases. Load case 1.5 is defined by power production plus extreme wind shear (EWS). Load case 2.3 stands for power production plus fault and extreme operation gust. Within the load case 2.3 two different gusts are used: The 1-year return gust (EOG_1_R) and the 50-year return gust (EOG_50_R). The approach is as follows:

First we created winds by using the provided input file which we adopted to our turbine and running the IECWind.exe. As mentioned in the task description only three of the set of generated files will be used: EOG_01_R.wnd, EOG_50_R.wnd" and EWSV00_R.wnd. Next the .ipt and .fst input files are adopted to our turbine and the generated wind files. Then the supplied Matlab script is used to derive results from the FAST output files.

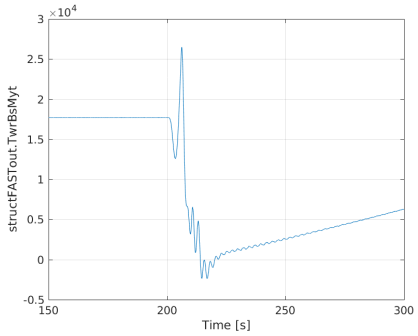

(a) Tower fore-aft for EOG_50

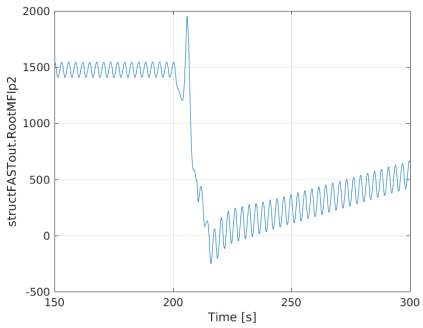

(b) Blade flapwise for EOG_50

Figure 29: Time series EOG

Let us have a look at the time series now. For load case 2.3 we consider the same sensors as in the fatigue analysis (tower fore-aft and blade flapwise bending moments) for the 50-year return gust, see Figure 29. With the occurrence of the gust and the failure a high peak in both signals follows and after that a steep decrease to zero with some oscillations and then a slow recovering of the signal. The reaction of the controller accounts for this behavior, because it changes the pitch angle in order to cope with the gust, see Figure 30.

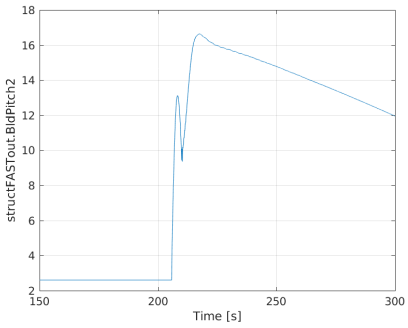

Figure 30: Pitch for EOG_50

The signals for the 1-year return gust look similar (here a gust of +4.5m/s is simulated instead of +6m/s as in the case of the 50-year gust).

For load case 1.5 we obtain the signals in Figure 31.

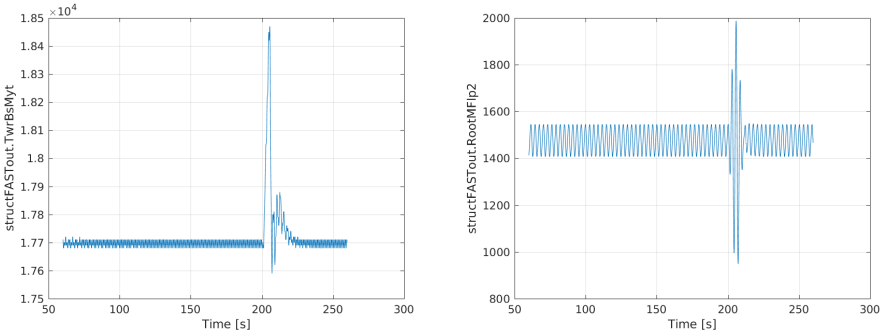

(a) Tower fore-aft for EWS (b) Blade flapwise for EWS

Figure 31: Time series EWS

Here we note that the extreme shear event also causes a peak in the signals, which is however especially for the tower not as high as in the case of EOG. Also recovery of the signal is much quicker: After only about 10 seconds the signals have returned to normal oscillations as before the extreme event. Likewise the controller reacted by adapting pitch angles of the blades in order to reduce power and loads due to the extreme shear.

No impact could be found regarding the timing of the failure except a shift of the event on the timescale. Concerning the influence of the brake we modified the input parameters a little. Activation time and time for nominal torque of the brake were considerably reduced (about 25%) while the nominal torque of the break was increased (around 20%). The recovery of the signal now goes much faster, see Figure 32. Here the signal already drops back to the values before the event at around $t = 300s$ whereas with the original brake settings this process takes approximately twice as long (compare Figure 29.

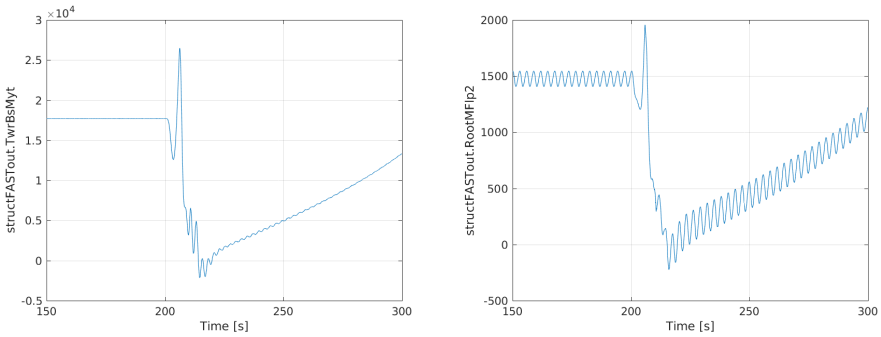

(a) Tower fore-aft (b) Blade flapwise

Figure 32: Modified breaks for EOG_50

A change in the time of the failure (TimeGenOf in the input file) does also affect the signal. We have had the failure occur before the extreme gust. The corresponding signal can be found in Figure 33. After the failure the signal drops to zero and then the gust appears and the return to normal operation of the turbine starts.

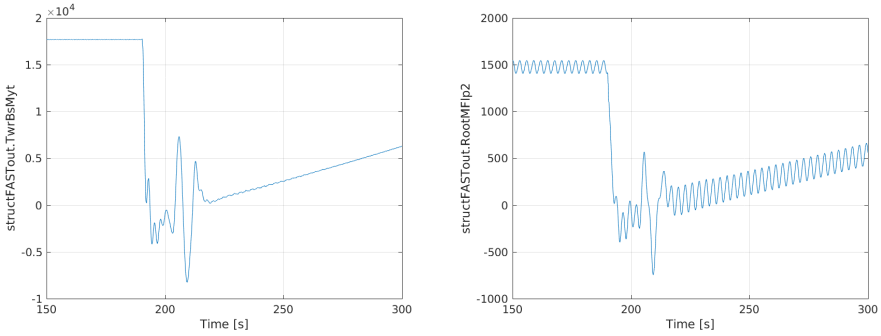

(a) Tower fore-aft (b) Blade flapwise

Figure 33: Changed failure time for EOG_50

8.3 Extreme load table

Group	Variable	Min/Max	DLC 1.5 EWS	DLC 2.3 EOG01	DLC 2.3 EOG50
Tower base	Fx	Min	206.9	-36.4	-20.01
Tower base	Fx	Max	219.5	326.5	324.8
Tower base	Fy	Min	-10.1	-56.23	-59.6
Tower base	Fy	Max	1.61	49.4	47.23
Tower base	Fz	Min	-2002	-2000	-2001
Tower base	Fz	Max	-1993	-1969	-1971
Tower base	Mx	Min	630.9	-1680	-2084
Tower base	Mx	Max	1630	2216	2567
Tower base	My	Min	17590	-3825	-2380
Tower base	My	Max	18470	26580	26490
Tower base	Mz	Min	-47.01	-114.7	-115
Tower base	Mz	Max	158.4	65.48	67.85
Blade root	Fx	Min	51.93	-7.054	-2.584
Blade root	Fx	Max	99.58	97.53	101.2
Blade root	Fy	Min	-53.65	-53.05	-53.83
Blade root	Fy	Max	28.19	38.35	38.11
Blade root	Fz	Min	196.9	184	186.2
Blade root	Fz	Max	281.2	339.1	337.6
Blade root	Mx	Min	-296.2	-470.9	-465.8
Blade root	Mx	Max	726.5	684.5	710.5
Blade root	My	Min	947.5	-277.6	-185.3
Blade root	My	Max	1966	1839	1943
Blade root	Mz	Min	0.7765	-0.4313	-0.4882
Blade root	Mz	Max	12.05	16.25	13.77

Table 11: Extreme load table

For tower base and blade root all max and min values of the 6 variables have been extracted from the signal data in Matlab. Values are in KN (forces) and kNm (moments). The first observation is that load case 2.3 dominates load case 1.5 with respect to the amplitudes. The more extreme values of the time series occur in the last and before-last column of the table. Only for some variables we find higher amplitudes for load case 1.5, e.g. TwrBsFzt and TwrBsMzt. Within the load case 2.3 there is no clearly dominant setting. The 1-year gust and the 50-year gust setting both have similar amplitudes in the signals. Sometimes EOG_01 has lower min or higher max values and sometimes EOG_50 wins.

9 Summary

In this design project the entire process of designing a wind turbine has been carried out. We have seen that it is a very complex undertaking requiring a lot of expertise from engineering, physics and also meteorology. The team has to be very accurate at any point and take into account a lot of aspects. The site conditions must be investigated in order to find out about the possible revenues of the turbine and thus the financial revenue during its lifetime. Economic feasibility is the pre-condition of the whole project for all stakeholders. The wind distribution, the design of the rotor blade and the mechanical and electrical efficiency must be taken into account. Wind turbine dynamics are an important aspect as well. Many design decisions must be met which influence the possible energy gain and also the further design process. Security is the next big topic. A load analysis has to be carried out regarding fatigue and extreme loads, otherwise the turbine can not be certified. All these steps and many more which have not been treated in this project require a professional team and a good time-management in order to successfully design a good turbine.